FEATURE ARTICLE

Ions at the Air/Water Interface

Pavel Jungwirth*,†,§ and Douglas J. Tobias*,‡,||

J. Heyrovský Institute of Physical Chemistry, Academy of Sciences of the Czech Republic and Center for Complex Molecular Systems and Biomolecules, Dolejškova 3, 18223 Prague 8, Czech Republic, and Department of Chemistry and Institute for Surface and Interface Science, University of California, Irvine, California 92697-2025

Received: January 24, 2002; In Final Form: March 25, 2002

We present results from theoretical studies of aqueous ionic solvation of alkali halides aimed at developing a microscopic description of structure and dynamics at the interface between air and salt solutions. The traditional view has depicted the air/solution interface of simple electrolytes as being devoid of ions. However, it is now firmly established that polarizable anions, such as the heavier halides, occupy the surface of small to medium sized water clusters. Using a combination of theoretical calculations, including ab initio quantum chemistry, Car−Parrinello molecular dynamics simulations, and primarily molecular dynamics simulations based on polarizable force fields, we present a unified view of the interfacial structure of aqueous ionic clusters and bulk solutions. Indeed, we demonstrate that the heavier halogen anions have a propensity for the interface that is proportional to their polarizability. The cluster results are directly supported by existing experimental and theoretical studies, and the bulk solution results are indirectly supported by several recent experiments. The novel view of the ionic solution/air interface presented here has also implications for dynamics following photoexcitation and electron photodetachment of ions. Moreover, the present results provide insight into heterogeneous atmospheric chemistry leading to halogen release from sea salt aerosols in the lower marine troposphere and from the Arctic snowpack during polar sunrise.

I. Introduction

There are no atomic ions at the air/solution interface of aqueous solutions. At least this has been the conventional wisdom for much of the twentieth century. The traditional view of an ion-free interface, which may be found in textbooks on surface and interface science,[1−4] is based exclusively on measurements of macroscopic properties of the surface.[4] Direct experimental verification that the aqueous solution/air interface is devoid of atomic ions has remained elusive because of the difficulties inherent in measuring the structure and/or composition of the highly disordered, inhomogeneous interfacial region of a liquid that has the thickness of a few water molecules at most.

The macroscopic property used most commonly to infer the composition of liquid/gas interfaces is the surface tension. The surface tension of the air/water interface is generally modified, and can be either increased or decreased, by a dissolved substance. Surface active agents ("surfactants," e.g. amphiphilic molecules such as alcohols and fatty acids) that adsorb to the air/water interface of aqueous solutions typically reduce the surface tension relative to that of pure water.[3] In contrast, inorganic electrolytes (e.g. alkali halide salts) typically increase the surface tension of the aqueous solution/air interface.[3] The extent of the surface tension modification depends on the nature and quantity of solute present in the interfacial region. The quantitative connection between the concentration of solute and the surface tension is derived from the Gibbs adsorption equation.[5] According to the Gibbs adsorption equation, the increase in surface tension with concentration of inorganic electrolyte corresponds to negative adsorption of the ions, i.e., the ion concentrations in the inhomogeneous interfacial region are less than in the bulk solution.[3] By extending the Debye−Hückel theory of electrolytes to the solution/air interface, Onsager and Samaras derived an equation that predicts the observed increase in surface tension with electrolyte concentration, and explained the negative adsorption in terms of repulsion of ions from the surface by electrostatic image forces.[6]

While experimental measurement of the microscopic structure of aqueous interfaces is difficult, it is relatively straightforward to predict structure, dynamics, and thermodynamic properties of liquid interfaces on the molecular scale using molecular dynamics (MD) simulations. MD simulations consist of numerically integrating the classical equations of motion for a system of particles, given a prescription for calculating the interparticle forces. Thus, MD simulations provide the ultimate detail in the form of a phase space trajectory for the collection of particles simulated. About a decade ago, MD simulations were first employed to study the adsorption of atomic ions to the air/water interface.[7,8] Strictly speaking, all of the solution/air interfaces modeled in the simulations described in this article are actually

* To whom correspondence should be addressed.
† Heyrovský Institute of Physical Chemistry.
§ E-mail: jungwirt@jh-inst.cas.cz.
‡ Department of Chemistry and Institute for Surface and Interface Science.
|| E-mail: dtobias@uci.edu.

10.1021/jp020242g CCC: $22.00
Published on Web 05/25/2002

solution/vacuum interfaces. In air at atmospheric pressure, the density of nitrogen, which is the most abundant component, is approximately 10^{19} molecules/cm^3. In the simulations, typically a 30 Å^3 slab of solution is placed in a 30 × 30 × 100 Å^3 box. From the free volume of the simulation box, and the density of nitrogen in air, it can be estimated that there should be less than one nitrogen molecule in the box to explicitly model the solution/air interface at atmospheric pressure. This is negligible, and therefore, the simulated solution/vacuum interface is regarded as a reasonable model for a small patch of solution/air interface.

In the pioneering MD simulations mentioned in the previous paragraph,[7,8] the interactions between the atoms were modeled by pairwise additive Lennard-Jones and Coulomb potentials, with fixed charges (partial charges on the water oxygen and hydrogen atoms, and full charges on the ions). Using the umbrella sampling technique, the free energy change associated with moving an ion from the bulk to the interface was computed. Although the quantitative details depended on the charge and size of the ions, both studies found that the surface location of cations (Na^+ and a positively charged ion with the Lennard-Jones parameters of a chloride anion), as well as anions (F^- and Cl^-) was energetically unfavorable by several kcal/mol compared to bulk solvation. Thus, these early simulations appeared to confirm the prevalent view that atomic ions have negligible populations at the solution/air interface. Detailed analysis of the simulations suggested that the tendency of the ions for negative adsorption was associated with weaker and fewer long-range interactions in the interfacial region compared to the bulk.[7]

The first indication that some atomic ions, for example the heavier halide anions, could actually be present at the air/water interface has come from cluster studies, both theoretical and experimental. Cluster systems are not only interesting in their own right, but also, by gradually extending the system size, may provide an insight into the properties of extended systems. At the same time, more accurate calculations can be performed, and better resolved spectra are usually obtained for clusters compared to bulk systems. An aqueous first solvation shell around a halide anion contains typically six to nine water molecules, depending on the particular anion. Also, one needs about six waters in order to distinguish between an interior and surface located ion. Therefore, we exclude from our discussion the large body of studies concerning the structure of small water−halide clusters with less than six water molecules.[9−19]

Molecular dynamics simulations that first predicted surface solvation of an atomic ion were performed for clusters containing the chloride, bromide, or iodide anion with mostly less than 20, but in one case with up to 255 water molecules.[20−31] The propensity of the heavier halogen anions for the surface of aqueous clusters has been contrasted to the behavior of the sodium cation[20] and fluoride anion,[23] which both reside in the interior of larger water clusters. By comparing simulations employing polarizable or nonpolarizable force fields, it has been shown that the driving force for surface solvation of chloride is the polarizability of the anion.[20,27,28] This is apparently the reason why aqueous surface solvation had not been observed for chloride in previous simulations employing nonpolarizable force fields.[7,8] The crucial role of ion polarizability in surface solvation also explains why hard, nonpolarizable ions such as the sodium cation or fluoride anion are repelled from the interface and prefer interior solvation, in accord with the classical Onsager−Samaras model derived for point charges.[6]

The cluster MD simulations discussed in the previous paragraph were motivated in part by photoelectron spectroscopy experiments on size selected water clusters containing the chloride, bromide, or iodide anion, with up to 60 solvent molecules.[32−34] Good agreement on binding energies between simulations and experiments was obtained, and it has been concluded, after a lengthy discussion, that the heavier halide anions do indeed reside at the surface of larger water clusters. The preference for surface solvation of chloride anion in aqueous clusters has been confirmed more recently by numerous calculations. On the side of small clusters (water hexamer) accurate ab initio calculations have been performed, as well as a Car−Parrinello molecular dynamics simulation.[35−37] Most recently, an ab initio molecular dynamics technique where the density matrix is propagated with Gaussian orbitals has been developed and applied to the $Cl^-(H_2O)_{25}$ cluster.[38,39] In the latter calculations, however, longer simulation times than the 50−200 fs achieved thus far are needed before questions concerning the location of the anion can be addressed. On the side of large clusters, MD simulations including many-body interactions via the so-called NEMO potential[40] or using the fluctuating charge model[30] have been performed for chloride on clusters with up to several hundreds of water molecules, showing again the propensity of polarizable ions for the surface.

Both theory and experiment have definitely converged on the conclusion that the polarizable, heavier halide anions reside on the surface rather than the interior of water clusters. Thus, as of the end of the twentieth century, the consensus was that the interfacial propensity of halide ions in clusters is decidedly different from that in bulk solutions, where the longstanding picture has the ions confined in the interior of the solution to within one or a couple of layers of water molecules from the surface. The apparent fundamental difference between halide ion solvation in clusters and extended liquid surfaces was recently discussed by Stuart and Berne in a paper in which they used a geometric model to rationalize the difference for a single chloride ion in terms of interfacial curvature.[30]

Recent experiments seeking to elucidate the role of halide anions in the atmospheric chemistry of sea salt aerosols have provided indirect evidence which suggests that the solvation of halide ions at extended liquid interfaces may have more in common with clusters than previously believed. For example, Hu et al. reported the enhanced reactive uptake of molecular halogens by the surfaces of halide solutions.[41] In another study, measurements of the kinetics of chlorine production by photochemically induced reactions of ozone with sea salt aerosols could not be explained by bulk phase chemistry involving chloride anions. However, a mechanism involving chloride anions at the aerosol solution/air interface was found to quantitatively reproduce the measured kinetics.[42] Using X-ray photoelectron spectroscopy and scanning electron microscopy, Ghosal et al. directly observed selective segregation of Br^- to the surface of bromide doped NaCl crystals under conditions of relative humidity where partial dissolution of the surface takes place.[43] The segregation of bromide to the surface is consistent with the conclusion from cluster studies that anion polarizability is a major factor determining the propensity of halide ions for the surfaces of aqueous clusters.

As we have indicated in the previous paragraph, the answer to the question of whether there are ions at the air/water interface has implications far beyond challenging established models of simple electrolytes. Heterogeneous atmospheric chemistry is probably the most eminent example. Indeed, both field and laboratory measurements indicate that aqueous sea salt aerosols

play an important role in the chemistry of the marine boundary layer.[42,44−51] There is increasing evidence that halide anions on the surface of these aerosol particles act as scavengers of reactive gases such as ozone or hydroxyl radical in the troposphere.[42,52] This represents a first step for a plethora of possible surface reactions, leading, e.g., to the release of molecular chlorine and other reactive halogen compounds into the atmosphere.

Another atmospheric process that evidently involves halide ions at an aqueous solution/air interface is bromine activation in sea salt aerosols or seawater spray deposited on the surface of polar ice packs. Field as well as laboratory measurements suggest that the photochemical release of Br_2 and BrCl is responsible for the destruction of the surface layer ozone in the Arctic at polar sunrise.[53−55] Similar bromine chemistry involving, albeit, lower mixing ratios of Br_2 and BrCl, is anticipated also in midlatitudes.[56]

While most of the processes involving halide anions at the air/water interface occur in the ground electronic state of the ion, there has been also recent interest in excitation of aqueous halide anions by UV radiation and following the subsequent dynamics. The dynamical processes involve interaction with light leading to photoexcitation of the anion to diffuse charge-transfer-to-solvent (CTTS) electronic states, or, for shorter excitation wavelengths, to electron photodetachment.

The CTTS bands corresponding to aqueous iodide anion had been observed already in the 1920s.[57] Since these early times, questions have arisen about the structure of the excited states and its relation to the appearance of the solvated electron. Recent time-resolved spectroscopic experiments,[58−60] as well as mixed quantum/classical molecular dynamics simulations,[61] show that a solvated electron is created by electron transfer from the excited anion into a nearby cavity site within 200 fs. These liquid studies are complemented by the advent of cluster experiments[62,63] and ab initio calculations[64−69] investigating the structure of the CTTS precursor states in finite size systems. A very recent computational study addressed the connection between the cluster and bulk liquid CTTS states with special emphasis on the air/water interface.[70]

As mentioned above, with a sufficiently energetic photon, direct electron detachment from the anion can be achieved. Provided the experiment is performed with high-resolution information can be gained about the ultrafast dynamics of the neutral system after electron photodetachment. Conventional photoelectron spectroscopy, such as that discussed earlier in this section, does not have such resolution. However, the negative ion zero electron kinetic energy (ZEKE) technique[71−74] provides spectral resolution approaching 1 cm^{-1} which is sufficient for studying the vibronic dynamics of the nascent neutral system. So far, experiments[75] and calculations[76,77] have been carried out only for the smallest halide anion−water complexes. However, studies of larger clusters are in progress.

In this paper we survey theoretical studies, based on molecular dynamics simulations and quantum chemical calculations, of aqueous halide ion solvation in interfacial settings (clusters and extended solution surfaces). Issues addressed here include the location and electronic structure of halide ions at aqueous interfaces, and the structure and dynamics of the hydration shell. While the focus is on our own calculations, some presented here for the first time, we also relate our results to available experimental data and previous theoretical investigations, and discuss their implications for the atmospheric chemistry of halide ions contained in sea salt. The rest of the paper is organized as follows. Section II summarizes the computational methodology. Section III presents results for halide ion/water clusters, while section IV deals with the interface of extended liquid systems with air. Section V discusses atmospheric applications, and section VI describes calculations and experiments concerning photoexcited surface solvated halide anions. Finally, concluding remarks are presented in section VII.

II. Methodology

The computational approach adopted for our study of ions at aqueous interfaces is a pragmatic mélange of ab initio quantum chemical techniques, Car−Parrinello type simulations, and classical molecular dynamics with a polarizable force field. The investigated systems are generally complex and large; therefore, there is little hope that numerically exact values could be obtained. Rather, we have aimed for consistency between the different computational approaches and for verifications of simpler methods against more sophisticated calculations on smaller systems, where the latter are still feasible. Whenever available, we have also validated the calculations by comparison to experimental data. Finally, we note that our main target has been the structural information, which is relatively robust in the sense that it is easier to reproduce by approximate calculations than, e.g., spectra.

A. Ab Initio Quantum Chemistry. Reliable ab initio calculations of aqueous atomic ions can be at present performed for no more than roughly 10 water molecules. For larger systems not only do the calculations become quickly prohibitively expensive, but mainly the exponentially increasing number of isomers prevents from a successful mapping of important points on the potential energy surface using standard quantum chemistry methods. An inherent problem of ab initio calculations is that they represent a 0 K description of the system under investigation. An easy, but also very approximate remedy is to include the effect of temperature within a simple harmonic oscillator/rigid rotor model. A more advanced approach, which is discussed below, is to account for temperature effect by a molecular dynamics sampling of the canonical ensemble.

In our study of sodium chloride in water hexamer,[78] we have employed for structure optimizations the second-order Möller−Plesset (MP2) perturbation theory with Pople's 6-31G* basis set augmented by a standard diffuse set on chloride, to capture the diffuse character of the valence shell of the anion. A very similar approach has also been adopted by other investigators for the study of chloride anion in clusters with up to six water molecules.[35] Comparison to calculations employing more extended basis sets or to methods including a larger portion of correlation energy (coupled cluster singles and doubles with perturbative triples) have shown a near-quantitative performance of the above approach. This is perhaps not surprising for systems that are held together by electrostatic forces, which can be accounted for accurately by using moderate basis sets and a modest treatment of electron correlation.

B. Classical Molecular Dynamics. Classical MD simulations with empirical force fields enable finite temperature phase space evolution and sampling for many-body systems. Presently, simulations covering nanonsecond time scales of aqueous systems consisting of thousands of atoms are routine. In simulations of aqueous ionic solutions, the heavy atoms are modeled as Lennard-Jones spheres, with full or partial charges located on or near the centers of all the atoms. As mentioned above, early simulations of ionic solutions employed force fields with fixed charges, but careful comparison of simulation and experimental results on ion−water clusters has clearly demonstrated that explicit inclusion of electronic polarizability is required for correct modeling of halide ion−water interactions.

There are various ways to incorporate polarization into the force field. The approach used most commonly thus far is to assign each atom an isotropic polarizability from which an induced dipole arises in response to the electric field produced by the remainder of the atoms in the system.[20,79] The induced dipoles are determined self-consistently by an iterative procedure or by an extended system method, and are used to calculate the polarization energy and forces at each time step. The induced dipole paradigm has been used extensively in simulations of ion−water clusters that have been validated by comparison to experimental data,[23,25,26,80] and we have used it in the simulations of the aqueous clusters and solutions reported in this paper. Another model that has seen relatively limited application, but appears to give similar results to the induced dipole model for chloride−water clusters, is the fluctuating charge model,[29,30] where the charges on the water atoms are fluctuating dynamical variables, and the polarizability of the chloride ion is described by a Drude oscillator.

As was pointed out in the Introduction, and as will be clearly demonstrated below, the propensity of halide ions for aqueous interfaces depends sensitively on the polarizability of the ion. Thus, for accurate quantitative predictions, it is important to employ appropriate values of the ion polarizabilities in force fields. It is well-known that halide ion polarizabilities are significantly reduced in condensed phases (e.g. crystals, solutions) compared to the gas-phase.[81,82] However, there have been no direct measurements of halide ion polarizabilities in aqueous solutions, and values used in simulations are extrapolations from ionic crystals and molten salts.[81,82] We recently used ab initio quantum chemical calculations to estimate the polarizability of the chloride ion on aqueous clusters, in bulk water, and at an extended liquid water/air interface.[83] The fields due to the water molecules were explicitly incorporated by placing point charges at the nuclear positions in cluster and liquid configurations obtained from energy minimizations and MD simulations. We found that, as expected, the water environment significantly reduced the chloride ion polarizability compared to the gas phase value. In the clusters the ion polarizability depended strongly on the particular geometry, while in the extended liquid system, the polarizability showed only a slight reduction as the ion was moved from the air/water interface to the bulk. The calculations suggested that a single value for the chloride ion polarizability of around 4 Å^3 is appropriate in aqueous environments. This is marginally higher than the range of values, 3.25 Å^3 to 3.76 Å^3, used in our own and other simulations of chloride−water systems,[20,27,30,42,83,84] indicating that the effect of polarizability might be even slightly larger than predicted in the above studies. Following Perera and Berkowitz[23] and Markovich et al.,[80] we have used values of 0.974, 4.53, and 6.90 Å^3 for the polarizabilities of F^-, Br^-, and I^-, respectively.

To model extended aqueous ionic solution/air interfaces, a slab of water molecules, doped with an appropriate number of ions to give the concentration of interest, is placed in the center of a rectangular box. The length of the box in the inhomogeneous direction is chosen to be much longer than the thickness of the slab, which in turn is large enough to leave a region of bulk solution in the interior. Periodic boundary conditions are applied in three dimensions, producing an infinite stack of planar slabs, each with two liquid/vacuum interfaces, following equilibration. In our calculation, the smooth particle mesh Ewald sum is used to evaluate the long-range electrostatic energies and forces.[85]

C. Ab Initio Molecular Dynamics. Ab initio MD simulations combine the advantages of electronic structure calculations, i.e., a description of interatomic interactions based on first principles, and classical MD simulation, namely, finite temperature sampling of phase space. Thus, electronic polarization effects are naturally included in fluctuations of the electronic structure. In ab initio MD simulations the nuclei are treated as classical particles, and their positions are evolved in time using standard MD simulation algorithms with forces computed from the electronic structure. In the most common implementation of ab initio MD, due to Car and Parrinello,[86] the nuclear positions and electronic orbitals are simultaneously evolved by an extended system method in which the orbitals undergo fictitious dynamics. When the simulation is started from a well-optimized wave function, and the orbitals are assigned light masses and are kept at very low temperature, the electronic degrees of freedom move adiabiatically on the Born−Oppenheimer surface defined by the nuclear configuration. Thus, the need to reoptimize the wave function for each nuclear configuration is circumvented.

In most applications to-date, including the one reported below, the electronic structure is computed within the Kohn−Sham formulation of density functional theory (DFT),[87] expanding the Kohn−Sham orbitals in a plane-wave basis set, treating only the valence electrons explicitly, and using norm-conserving pseudopotentials to describe the valence-core interactions.[88] The efficiency of the Car−Parrinello technique and the plane-wave based DFT electronic structure calculations makes it presently feasible to simulate systems with tens of heavy atoms for several picoseconds. Quantitatively correct structures and energetics, as well as reasonable results for the dynamics have been obtained for a variety of aqueous systems[36,89−91] using modest sized plane-wave basis sets (e.g., expanded to an energy cutoff of 70 Ry) and the gradient-corrected BLYP exchange−correlation functional.[92,93]

III. From Small to Large Clusters

A. Onset of Ionic Solvation In/On Small Water Clusters. Cluster systems represent a convenient ground for studying the onset of aqueous solvation around an ionic impurity. The water hexamer is about the smallest system where surface vs interior solvation of an ion can be clearly distinguished. At the same time, the cluster is small enough to allow for performing accurate ab initio calculations. Therefore, it serves as an ideal benchmark for testing force field MD simulations against quantum chemical and ab initio MD simulations. Last but not least, experimental data concerning binding and electron affinity are available for this system from photoelectron spectroscopy measurements.[34]

In a recent study,[36] we performed an ab initio Car−Parrinello MD simulation of the $Cl^-(H_2O)_6$ complex at 250 K. The performance of the DFT electronic structure method commonly employed for aqueous systems was validated by a favorable comparison to MP2 results for the structures and energetics of adding water molecules to minimum energy geometries of $Cl^-(H_2O)_n$, $n = 1-4$, clusters. The ab initio simulation was initiated from a configuration, taken from a MD simulation of the cluster with a nonpolarizable force field, in which the chloride anion was in the interior of the cluster, well-solvated by all six water molecules. Within approximately 0.5 ps the ion moved to the surface of the cluster, where it stayed for the rest of the 5 ps simulation. The evolution of the structure of the complex, and the distance of the anion from the center-of-mass of the cluster, are shown in Figure 1. Several structural properties of the cluster computed from the ab initio simulation were found to be in good agreement with predictions based on polarizable force fields.

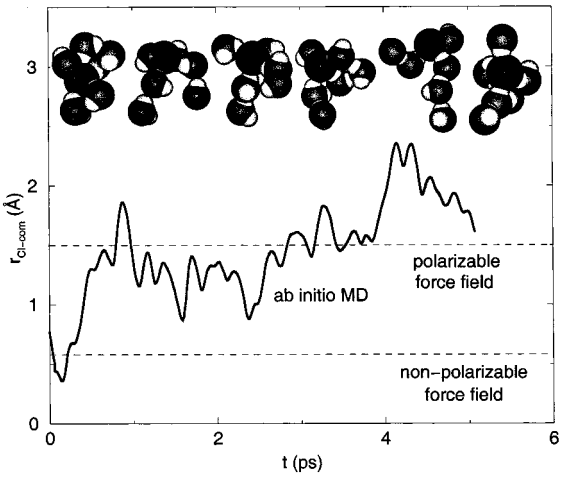

Figure 1. Time evolution of the distance between the chloride anion and the cluster center-of-mass during an ab initio MD simulation of $Cl^-(H_2O)_6$ at 250 K. The dashed horizontal lines indicate the average values computed during MD simulations based on polarizable and nonpolarizable force fields. Also shown are snapshots from the ab initio simulation from 0 to 5 ps at 1 ps intervals.

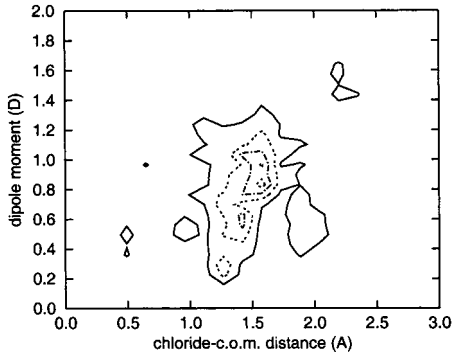

Figure 2. Contour plot of the joint probability distribution of the distance between the chloride anion and the cluster center-of-mass (horizontal axis) and the chloride dipole moment (vertical axis) from a 5 ps ab initio MD simulation of $Cl^-(H_2O)_6$.

One of the attractive features of an ab initio simulation is the natural description of fluctuations of the electronic structure that accompany finite temperature sampling of the nuclear degrees of freedom. We quantified the evolution of the electronic structure during the ab initio simulation in terms of the centers of maximally localized orbitals (Wannier functions).[94,95] The analysis revealed that the chloride ion sampled a broad distribution of dipole moments as the structure of the cluster fluctuated, with an average of about 0.8 D. This modest average dipole moment is a manifestation of the asymmetric solvation of the anion, which resided primarily on the surface of the cluster. A correlation between the polarization of the chloride ion and the asymmetry of the hydration shell may be seen in Figure 2, where it is evident that larger chloride dipole moments are generally associated with larger distances between the anion and the center-of-mass of the cluster.

Another study concerning ions in/on water hexamer has dealt with the onset of NaCl solvation in aqueous clusters.[78] The following questions have been addressed: (i) What is the minimal number of water molecules necessary for ionic solvation, i.e., for creating a solvent-separated ion pair? (ii) What are the solvation sites (surface vs interior) of the two ions? (iii) Can bulk values be extrapolated down to finite size systems?

The answer to the first question has been obtained by a back-of-the-envelope estimate of the relative stabilities of a contact and solvent-separated NaCl ion pair in small water clusters,

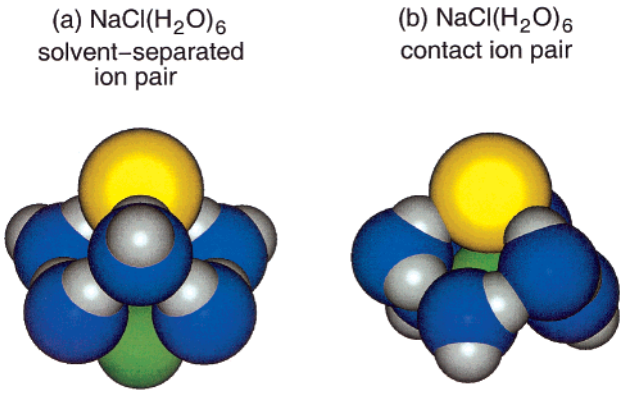

Figure 3. Minimum energy geometries of $NaCl(H_2O)_6$: (a) solvent-separated ion pair; (b) contact ion pair. Coloring scheme: chloride anion, yellow; sodium cation, green; water oxygen, blue; water hydrogen, gray.

followed by an extensive ab initio scan of relevant portions of the potential energy landscapes of the clusters. It has been found that water hexamer is the smallest aqueous cluster which can stabilize a solvent separated ion pair. A secondary minimum, corresponding to the unsolvated NaCl molecule (contact ion pair) and separated from the solvent separated ion pair by a barrier of more than 4 kcal/mol, has also been located. The geometries of the two nearly isoenergetic isomers are shown in Figure 3.

It is immediately clear from Figure 3 that the two structures are qualitatively different. The solvent separated ion pair with Na−Cl distance of 4.43 Å has the two ions surface solvated on opposite sides of the water cluster. Note, also, that the individual dipoles of the water molecules are almost perfectly aligned along the electric field between the ions with very little residual water−water hydrogen bonding. On the other hand, the contact ion pair with a Na−Cl bond length of 2.66 Å has sodium embedded in the water cluster, while chloride remains at the surface. The water structure with almost intact hydrogen bonds is much less disrupted by the solute than in the previous case.

It is interesting to compare the obtained minimal number of six waters for NaCl solvation to previous predictions. A simple extrapolation from the bulk liquid based on saturation concentration gives nine water molecules.[96] Calculation based on a continuum solvent model and employing the potential of mean force between the two ions from an MD simulation predicts 12 waters as a minimal cluster size for ion separation.[97] Clearly, extrapolation from the bulk is quantitatively wrong and one has to go beyond the continuum model of the solvent in order to obtain quantitative results. Interestingly, a study of NaCl in water clusters with up to 10 water molecules based on the effective fragment potential approach did not lead to the location of a solvent separated ion pair.[98] However, the authors recently found that starting from the solvent separated structure presented in Figure 3 they were indeed able to stabilize a geometrically very similar solvent separated ion pair using effective fragment potentials.[99] It is fair to conclude by stating that the present results are robust and nearly converged computationally; however, direct experimental confirmation of the fact that no more than six waters are necessary to dissolve a NaCl molecule is still missing.

B. Ionic Solvation In/On Large Water Clusters. To bridge the gap between the studies concerning ions in/on a water hexamer on one side and ions at the air interface of the bulk liquid on the other side, we have launched a series of MD simulations on clusters of increasing size.[42] Namely, we have investigated clusters containing 9−288 water molecules, doped

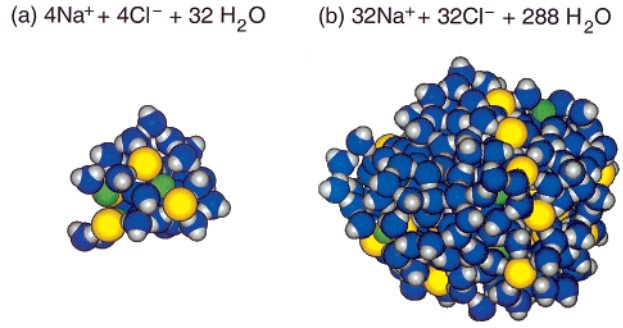

Figure 4. Snapshots from MD simulations of sodium chloride−water clusters: (a) $(NaCl)_4(H_2O)_{32}$ and (b) $(NaCl)_{32}(H_2O)_{288}$. The coloring scheme is the same as that in Figure 3.

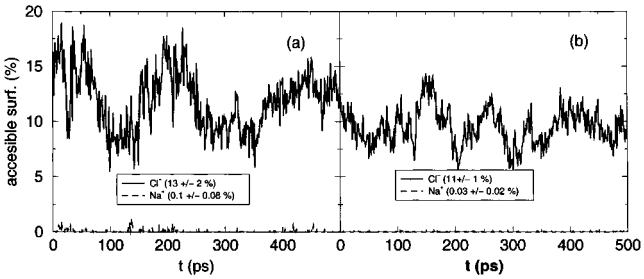

Figure 5. Time evolution fraction of area occupied by sodium (broken curves) and chloride (solid curves) ions on the surface of sodium chloride−water clusters (snapshots shown in Figure 4): (a) $(NaCl)_4(H_2O)_{32}$ and (b) $(NaCl)_{32}(H_2O)_{288}$.

with sodium chloride. For all systems, the salt concentration has been fixed at the bulk saturation value under ambient conditions of 6.1 M, corresponding to nine water molecules per sodium chloride. We discuss here the results for a small cluster containing 32 waters, 4 sodium cations, and 4 chloride anions, and a large cluster with 288 waters, 32 sodium cations, and 32 chloride anions.

Typical snapshots of the two systems from MD runs are depicted in Figure 4. It can immediately be seen that in both cases large polarizable chloride anions are to a significant extent exposed at the surface of the clusters, while the small nonpolarizable sodium cations tend to be embedded within the waters. This effect can be quantified in two ways. The first possibility is to calculate density profiles, i.e., averaged probability of finding ions of a certain type at a specific distance from the center of the cluster. This proves to be a very useful quantity for interfaces of bulk liquid systems. However, in clusters, the protrusion of ions is masked by the highly fluctuating shape (nonsphericity) and corrugation of the cluster surface. Therefore, we have found it more useful to calculate the averaged accessible surface for the two ionic species to a spherical probe[100] (results reported here were obtained using a probe with a radius of 1.7 Å which is roughly the size of an OH radical).

The time profiles during the simulation of the accessible surface area of ions in the two clusters are presented in Figure 5. There is a dramatic (2 orders of magnitude) difference between the two ions. Chloride anions occupy about 12% of the total cluster surface and are, in fact, comparably exposed as water molecules. Sodium cations are, on the other hand, practically absent from the surface. This effect is present both in small and large clusters and qualitatively does not depend on system size. We have also verified that within ± 20 K variations from the ambient temperature of 300 K, the surface effect is temperature independent. Finally, by switching to a nonpolarizable force field the surface exposure of chloride drops by a factor of 3, thus demonstrating yet again the dominant role of polarizability in determining the surface propensity of halide anions.

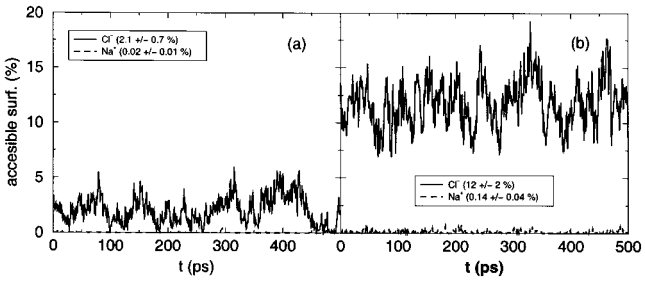

Figure 6. Time evolution fraction of area occupied by sodium (broken curves) and chloride (solid curves) ions on the surface of sodium chloride solutions: (a) 1.2 M and (b) 6.1 M. The average values and their statistical uncertainties are given in the legends.

IV. Slabs: Extended Air/Liquid Interface

Sea salt aerosol particles that participate in atmospheric chemical processes are much larger than the clusters that have been simulated and characterized at the molecular level experimentally. To investigate whether ionic solvation in sea salt aerosols is similar to that in smaller clusters we have performed a series of MD simulations of ionic solutions containing extended liquid interfaces, modeled using slabs as described above. Because sea salt aerosol particles have diameters on the order of microns,[47] the slabs are expected to be good models for local patches of the surfaces of the aerosol particles that are small enough for curvature effects to be negligible. The picture that has emerged from these simulations, which we have found to be in accord with a number of experimental results, is one in which the polarizable, heavier halide anions are present and available for direct reaction with atmospheric pollutants at the aerosol/air interface.

A. Water Slabs with Sodium Chloride. As part of a combined experimental and theoretical investigation of chlorine production by aqueous salt aerosols in the presence of photolyzed ozone (leading eventually to OH radicals), we performed MD simulations of a slab containing a saturated (6.1 M) solution of sodium chloride.[42] The kinetics of the chlorine production measured in the laboratory could not be modeled using known bulk phase chemistry. Simulations using a polarizable force field predicted that approximately 12% of the surface area of the aerosol particles was occupied by chloride anions (see Figure 6b). Incorporation of this estimate into a kinetic model that included novel interfacial reactions suggested by ab initio quantum chemical calculations led to excellent agreement with the measured kinetics. This provided strong evidence in favor of the simulation-based prediction that chloride anions have a propensity for the extended interfaces of aqueous solutions. We showed in the same study that, consistent with the cluster results presented in the previous section, the propensity of an anion for the interface is strongly tied to its polarizability. Indeed, using a nonpolarizable force field, the coverage of the extended solution interface by the chloride anion dropped to approximately 3%. It is worth noting that, for sodium chloride at high concentration (6.1 M), the composition of the extended solution interface is strikingly similar to that of the surfaces of moderately sized aqueous clusters (containing 36 −288 water molecules).

More recently, we have examined the concentration dependence of the interfacial properties of sodium halide solutions at three concentrations ranging from infinite dilution to saturation.[84] We found that the sodium cations remain well solvated in the interior of the solution while the chloride ions occupy a

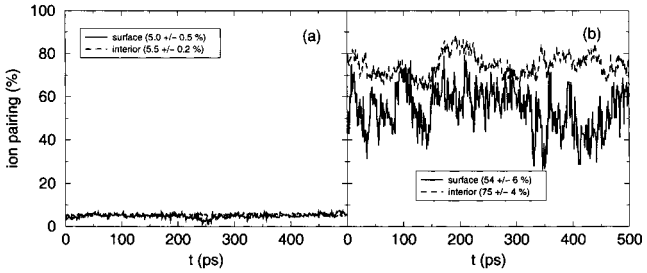

Figure 7. Time evolution of the extent of ion pairing exhibited by chloride ions near the surface (solid curves) and in the interior (broken curves) in sodium chloride solutions: (a) 1.2 M and (b) 6.1 M. The division between the surface and interface has arbitrarily been chosen as 1 Å toward the interior from the point where the water oxygen density begins to decay from its bulk value.[84] The average values and their statistical uncertainties are given in the legends.

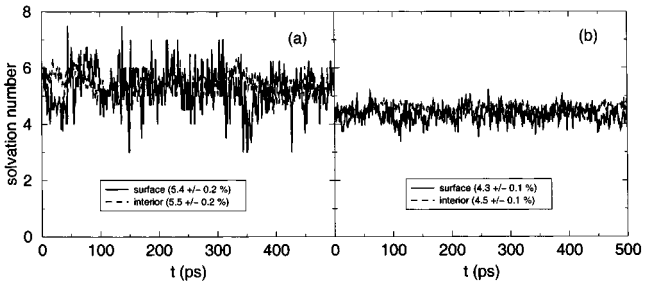

Figure 8. Time evolution of the number of water molecules in the first solvation shell of chloride ions near the surface (solid curves) and in the interior (broken curves) in sodium chloride solutions: (a) 1.2 M and (b) 6.1 M. The definition of the surface region is given in the caption to Figure 7. The average values and their statistical uncertainties are given in the legends.

significant fraction of the surface over the entire concentration range. As is evident from the results shown in Figure 6 for the 1.2 and 6.1 M solutions, the extent of the occupation of the surface by the chloride anions is proportional to the concentration, and is roughly constant over the duration of the simulations.

The reactivity of a halogen anion is expected to depend on the number and strength of the interactions between the anion and counterions and/or water molecules. We have attempted to assess the extent to which the reactivity of a chloride anion could be modified at the interface relative to the bulk by quantifying the anion−cation and anion−water interactions. In Figure 7 we compare the time evolution of the average extent of Na^+-Cl^- pairing in the interfacial region and bulk at 1.2 and 6.1 M NaCl. At 1.2 M the difference in ion pairing between the interface and bulk is small (5.0% vs 5.5%). However, at saturation 75% of the chloride ions are paired in the bulk compared to 54% at the interface. This suggests that in the aerosol particles consisting of a saturated NaCl solution, there is a significant amount of unpaired chloride anions. As unpaired anions are expected to be more reactive, this is in accord with the proposed participation of interfacial chloride in reactions with atmospheric gases.[42]

In Figure 8 we compare the time evolution of the average number of water molecules hydrating chloride anions. The average hydration numbers are 5.5 and 4.5 in the bulk at 1.2 and 6.1 M, respectively. These values should be compared to the chloride coordination number of 6.0 at infinite dilution. The hydration number drops with concentration due to an increase in ion pairing. The effect of incomplete solvation is reflected in the slightly smaller hydrations numbers in the interfacial region compared to the bulk.

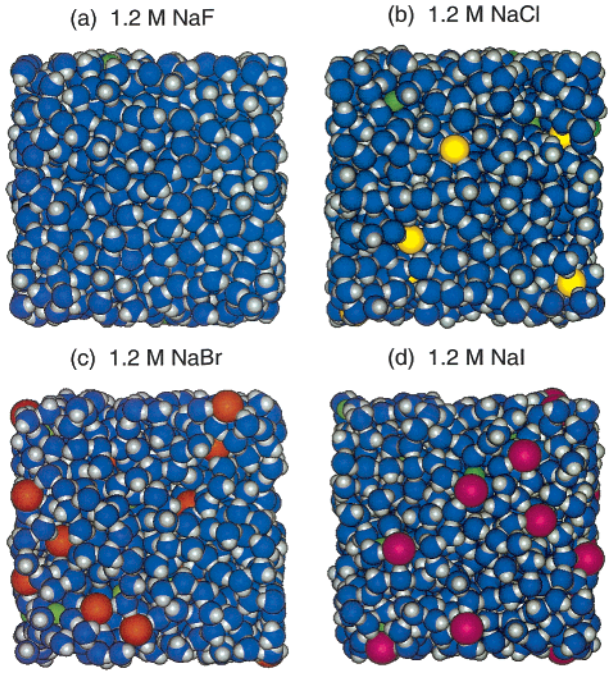

Figure 9. Snapshots viewed from the air side from MD simulations of the solution/air interfaces of 1.2 M sodium halide solutions: (a) sodium fluoride, (b) sodium chloride, (c) sodium bromide, and (d) sodium iodide. Coloring scheme: fluoride ion, black; chloride anion, yellow; bromide anion, orange; iodide anion, magenta; sodium cation, green; water oxygen, blue; water hydrogen, gray.

B. Comparison between Water Slabs with NaF, NaCl, NaBr, or NaI. To obtain a more complete picture of the behavior of specific anions at the air/water interface we have performed a set of simulations of aqueous slabs doped with sodium fluoride, chloride, bromide, or iodide at a 1.2 M concentration in all four cases.[83] One of the primary purposes of the study was to see if we could reproduce the experimentally observed modifications of the surface tension by the sodium halide salts. Indeed, we found that, in agreement with experimental observations, simulations of all of the sodium halide solutions resulted in a slight increase (less than 10%) in surface tension relative to pure water. Remarkably, the simulations also correctly reproduced the order of the surface tension in the series: NaI < NaBr < NaCl < NaF: namely, the calculated increase of the surface tension with respect to pure water amounts to 2.8 mN/m (experiment gives 1.2 mN/m) for sodium iodide, 2.9 mN/m (exp. 1.6 mN/m) for sodium bromide, 3.4 mN/m (exp. 2.0 mN/m) for sodium chloride, and 5.1 mN/m (exp. 3.6 mN/m) for sodium fluoride.[83]

As was discussed in the Introduction, historically the increase of surface tension of inorganic electrolyte solutions has been interpreted via the Gibbs adsorption equation in terms of negative adsorption, i.e., the solution/air interface is devoid of ions. Analysis of the interfacial structure predicted by our simulations suggests that this interpretation is too simplistic. Snapshots from the simulations, viewed from the air side, are shown in Figure 9, and density profiles of the ions and water oxygen atoms are plotted in Figure 10. There are no ions visible in the snapshot from the simulation of the NaF solution, and the density profiles show that both the sodium and fluoride ions are repelled from the interface, leaving an ion-free layer approximately 3.5 Å thick. This is in accord with the classic theory of Onsager and Samaras,[6] and the agreement for the small, nonpolarizable sodium and fluoride ions is sensible. However, moving down the halide series (from chloride to

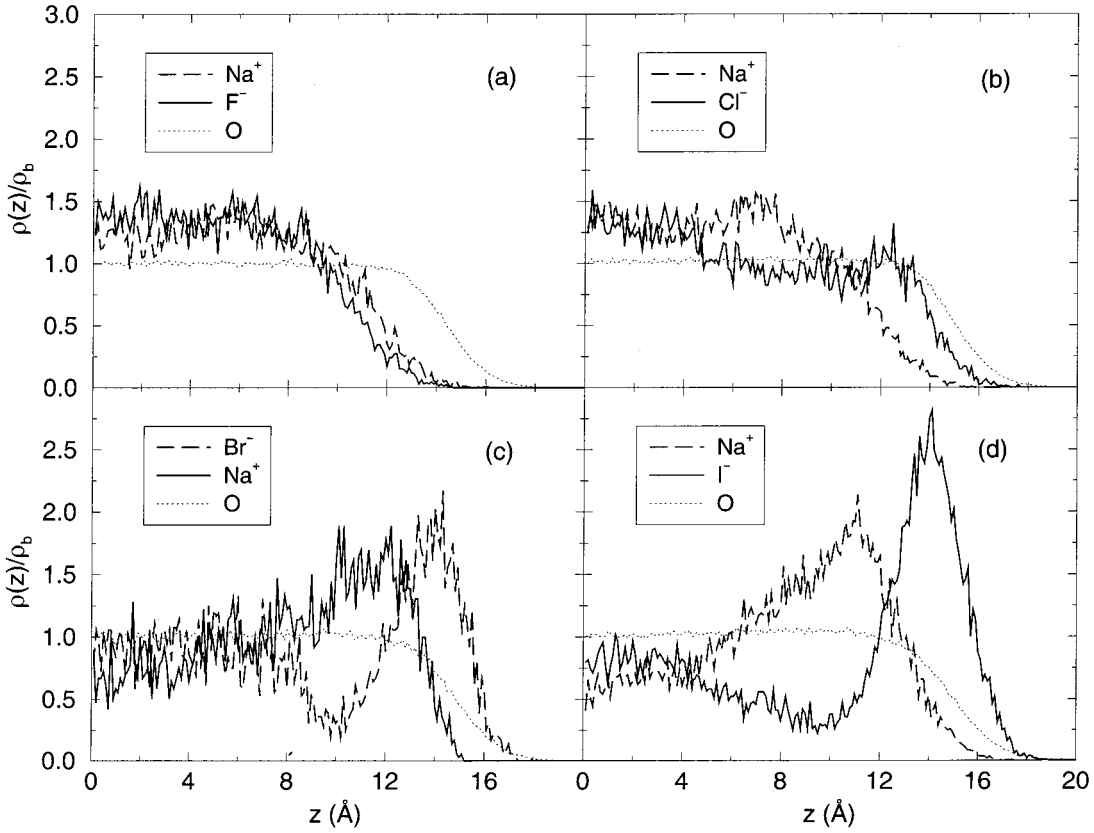

Figure 10. Number densities of water oxygen atoms and ions computed from MD simulations of 1.2 M sodium halide solutions plotted vs the distance (z) from the center of the slabs in the direction normal to the interface, normalized by the bulk water density, ρ_b: (a) sodium fluoride, (b) sodium chloride, (c) sodium bromide, and (d) sodium iodide. The ion densities have been scaled by the water/ion concentration ratio for ease of comparison.

bromide to iodide), we see an increasing population of the surface by the anions, tracking the increase in the anion polarizability. While the chloride anion is predicted to have some propensity for the interface, its concentration in the interfacial layer is still slightly below (by about 30%) the bulk concentration. In contrast, the bromide and iodide anions actually behave as surfactants, with concentration enhancements in the interfacial region relative to the bulk of 2.1 and 2.9, respectively. The density profiles can be directly converted into potentials of mean force using a Boltzmann relation $\Delta G(z) = -kT \log\rho(z)/\rho_b$ (see also Figure 10). For bromide and iodide, which exhibit a density peak at the interface this corresponds to an additional stabilization at the interface of roughly 0.5 and 0.8 kcal/mol, respectively. Our prediction for the iodide ion is consistent with a most recent simulation study of iodide in a water slab at infinite dilution, in which a minimum in the potential of mean force for moving the ion across the air/water interface was found at the interface.[101]

The additional stabilization of polarizable ions at the air/water interface can be qualitatively rationalized as follows. Upon asymmetric solvation at the surface the ion is subjected to a nonzero net dipole, which is the vector sum of the individual dipoles of the surrounding water molecules. Note that, in the bulk, this net dipole on average equals to zero due to a symmetric solvation of the ion. At the air/water interface the net water dipole polarizes the (polarizable) ion leading to an energy gain which can balance (or even overcome) the energy penalty due to uncomplete solvation.

C. Water Slabs with a Mixture of NaCl and NaBr. Questions that naturally arise in the context of atmospheric chemistry concern aqueous interfaces doped with more than one anionic species. As a practical example, we consider aqueous sea salt aerosols, which contain both chloride and bromide ions, in a molar ratio of approximately 650:1.[47] We have just completed a series of MD simulations of aqueous slabs doped simultaneously by sodium chloride and sodium bromide at various absolute and relative concentrations, and we present the first results below.

Closest to the atmospheric reality of aqueous sea salt microaerosols is a simulation of a slab with a unit cell containing 864 water molecules, 96 sodium cations, 95 chloride anions, and a single bromide anion. This corresponds to a saturated system with bromide concentration larger, but of the same order of magnitude as that occurring in the seawater. As a starting geometry, we have used a slab saturated with sodium chloride from our previous simulations and at $t = 0$ we have "transmuted" one of the chlorides into a bromide anion. Two 800 ps runs have been performed, the first with the bromide ion initially at the interface, and the second with the bromide ion initially in the slab interior. Figure 11 shows the variation of the distance of bromide from the center of the slab along the two dynamical runs. While fluctuations naturally occur, the emerging trend is clear. If bromide is initially placed at the interface (which corresponds to the distance of 15−19 Å from the center of the slab), it remains there for the whole duration of the simulation. However, if it is initially embedded in the slab, the bromide ion very rapidly, i.e., within 0.5 ns finds its way to the interface and remains there. The driving force is again the polarizability, which is about 30% larger for bromide compared to chloride.[80] The difference in ionic radii is much smaller and does not seem to play an important role.

To quantify the relative propensities of bromide vs chloride for the interface we have performed equilibrium MD simulations of two aqueous slab systems, one doped with 0.6 M of NaCl

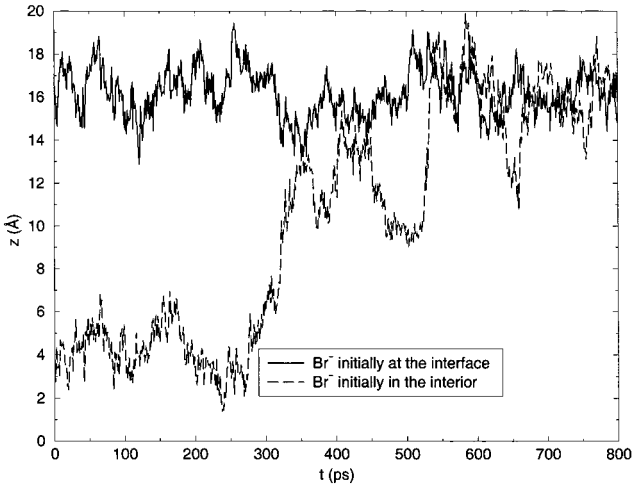

Figure 11. Position of a bromide anion as a function of distance (z) from the center of the slab in the direction normal to the interface in MD simulations of a 6.1 M sodium chloride solution in which the bromide ion was initially place near the solution/air interface (solid curve), and in the bulk solution near the center of the slab (broken curve).

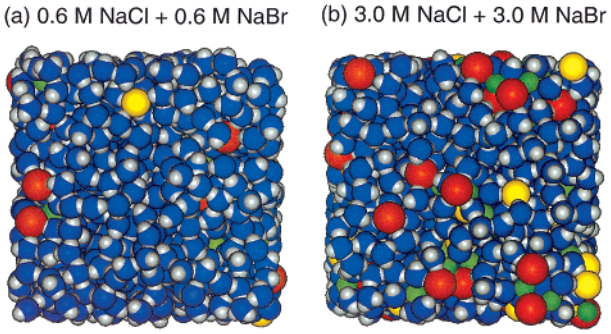

Figure 12. Snapshots viewed from the air side from MD simulations of the solution/air interfaces of aqueous solutions of mixtures of sodium chloride and sodium bromide: (a) 0.6 M sodium chloride + 0.6 M sodium bromide and (b) 3.0 M sodium chloride + 3.0 M sodium bromide. The coloring scheme is that same as that in Figure 9.

and 0.6 M of NaBr, and the other, more concentrated, containing 3 M of both NaCl and NaBr. Typical snapshots from each of the two simulations are depicted in Figure 12. They illustrate that, between the two anions, bromide is a clear winner over chloride in surface exposure. This is demonstrated quantitatively in Figure 13 which shows the density profiles of the three ions (Cl^-, Br^-, and Na^+) for the two systems. For both concentrations, we see a strong peak corresponding to interfacial positions of bromide. At the lower concentrations the ionic signals more or less add linearly, chloride being roughly evenly distributed in the slab and sodium cation being absent from the interface. The bromide concentration at the interface exceeds about twice its bulk value, while that of chloride reaches 90%, and that of sodium cations only 20% of the bulk value. The situation is quantitatively different in the more concentrated system where bromide anions replace virtually all the chlorides from the interface. To reduce the large interfacial negative charge, some sodium cations are dragged toward the surface. As a result, surface concentration of sodium cations reaches 80% of the bulk value, being thus higher than that of chloride (60%), although much smaller than that of bromide (320%). We conclude that, for higher concentrations, one cannot predict the properties of the mixture of NaCl and NaBr by simply extrapolating the results from single salt solutions, since nonlinear effect come into play.

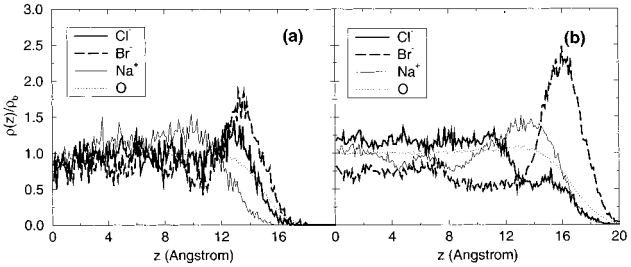

Figure 13. Number densities of water oxygen atoms and ions computed from MD simulations of aqueous solutions of mixtures of sodium chloride and sodium bromide plotted vs the distance (z) from the center of the slabs in the direction normal to the interface, normalized by the bulk water density, ρ_b: (a) 0.6 M sodium chloride + 0.6 M sodium bromide and (b) 3.0 M sodium chloride + 3.0 M sodium bromide. The ion densities have been scaled by the water/ion concentration ratio for ease of comparison. Sodium ion densities are plotted with thin solid curves, chloride anion densities with thick solid curves, bromide anion densities with thick dashed curves, and water oxygen densities with thin dotted curves.

There is indirect experimental evidence supporting the enhanced propensity to the interface of bromide compared to chloride from recent XPS and SEM surface measurements of solid NaCl/NaBr cocrystal particles.[43,47] It has been shown that the surface of these particles becomes strongly enriched with bromide upon exposure to water vapor and subsequent redrying. This demonstrates that if mobility is enabled by partial dissolution of the particles, bromide is pushed toward the interface, in agreement with the results of the MD simulations.

V. Atmospheric Applications

A prime application of the present results concerns atmospheric chemistry, in particular heterogeneous processes occurring in the lower marine troposphere. As a matter of fact, field and laboratory measurements of the reactivity of aqueous sea salt aerosols[42,44,45,47] originally motivated the theoretical research presented in this paper. Aqueous sea salt aerosols are created in abundance in the marine boundary layer by wave action and may represent a global tropospheric source of reactive halogens, such as molecular chlorine.[42,44]

It has been demonstrated in laboratory measurements that only four ingredients are essential for molecular chlorine production: dry sea salt aerosols (actually, sodium chloride suffices), humidity above deliquescence point, UV radiation, and ozone gas.[45] The proposed mechanism involves photolysis of ozone in humid air leading to peroxide, which further photolyzes producing OH radicals. The OH radicals were assumed to complex with chloride anions in the bulk of the submicron sized aqueous sea salt aerosol particles, and subsequently produce chloride radicals via charge transfer to aqueous protons. Chloride radicals could then produce molecular chlorine, either directly or by addition to Cl^- followed by a self-reaction of two Cl_2^- ions.[45]

The main problem with the above mechanism is that in roughly pH-neutral sea salt aerosols there are not enough aqueous protons for the charge-transfer step. This led to speculations about a reaction proceeding via a different mechanism—a direct charge transfer from Cl^- to OH on the surface of the aerosol particle. The present slab simulations showed that indeed there is a sufficient concentration of chloride anions at the interface for the surface mechanism to be a plausible one. Incorporation of the surface processes into a kinetic model lead to a quantitative reproduction of the laboratory measurements of the time-dependent concentrations

of ozone and chlorine in the aerosol chamber.[42] Moreover, agreement has been found also between predictions of the new kinetic model and field measurements of diurnal concentrations of Cl and OH radicals above the Southern Ocean.[42,102,103]

Aqueous sea salt particles are dispersed not only into the air but also on the surface of snow packs in the polar regions. This deposition, associated with air masses transported over sea ice and snow during polar winter, results in a sudden outburst of bromine reactivity at polar sunrise, leading to destruction of the surface ozone layer. Measurements show that bromine chemistry is strongly enhanced compared to the seawater Br:Cl molar ratio.[104−106] It is natural to assume that, similarly to the case of tropospheric aqueous sea salt aerosols, processes at the liquid surface of snow packs sprayed with seawater may play an important role.[55] The enhanced reactivity of bromine can then be rationalized in terms of the larger rate constant (compared to chlorine) combined with the increased relative (to chloride) and absolute propensity of bromide anions for the air/water interface, as observed in the MD simulations reported here.

VI. Dynamics Upon Photoexcitation

A. CTTS States of Iodide at the Air/Water the Interface. Investigations concerning UV photoexcitation of aqueous iodide to the charge-transfer-to-solvent (CTTS) states eventually leading to a solvated electron date back to early studies by Franck et al.[57] More recently, femtosecond experiments[58−60] as well as quantum/classical MD simulations[61] have shown that in the bulk liquid the CTTS states decay into a solvated electron located in a cavity site in a close vicinity of iodine within 200 fs. It has been shown recently via MD simulations that aqueous iodide exhibits surfactant activity[83] and several recent experiments have probed I^- at the air/water interface.[107,108]

In our most recent study[70] we have, among other things, investigated the character of the iodide CTTS states at the air/water interface. We have used the classical MD technique with a polarizable force field to sample representative slab geometries corresponding to the ground-state anion. Subsequently, we have performed ab initio second-order perturbation (MP2) and configuration interaction with single excitations (CIS) calculations for the ground and excited (singlet and triplet) states of the anion and ground state of the neutral system using geometries from the MD simulation. To make the ab initio calculations computationally feasible, we have replaced all water molecules (or all except for the first solvation shell) by fractional point charges. Quantitative agreement with experimental excitation and detachment energies has been obtained, including the widths due to the sampled statistics of water geometries.

Figure 14 depicts the CTTS wave function (i.e. the highest singly occupied molecular orbital) for a typical geometry of (ground state) iodide in water from the MD simulation. The CTTS orbital is very diffuse and occupies a void in the water structure next to iodine. Such temporary voids are always present in the liquid due to thermal disorder. The wave function possesses a radial node and is of a mixed s and p character.

A somehow surprising finding is that, unlike in small water clusters, the character of the iodide CTTS electron in liquid water does not change significantly upon moving the ion from the interface to the interior. Quantitatively, the CTTS electron is on average more strongly bound at the interface by only 0.26 eV, while the average value of this difference for the ground state of iodide is even smaller (0.1 eV). These small values can be partially explained by the longe-range liquid disorder which to a large extend smears out the difference between various solvation sites. Moreover, there is a large degree of binding energy compensation: surface solvated iodide loses binding to one or two water molecules in the first solvation shell, but this is compensated (actually slightly overcompensated) by a gain in induction energy due to asymmetric solvation in a polar solvent.[83]

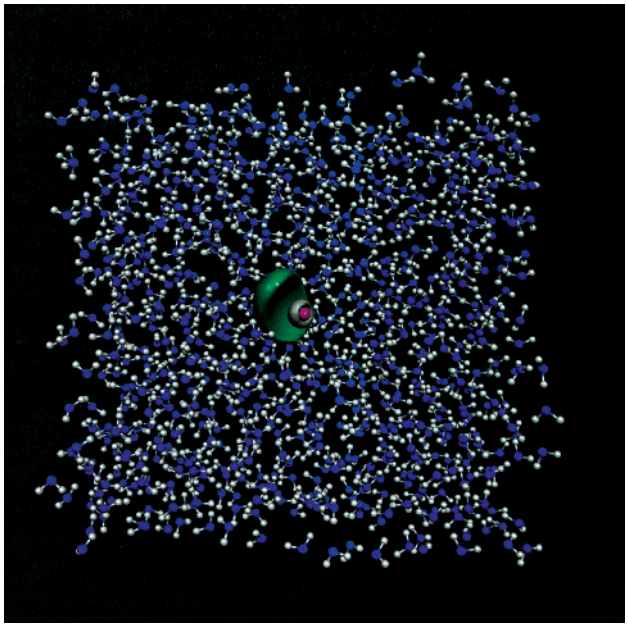

Figure 14. Typical shape of the CTTS wave function (i.e., highest occupied molecular orbital of the triplet CTTS state) for iodide (purple) at the air/water interface.

Another important conclusion of the recent study[70] is that the character of the CTTS states in the extended liquid environment is very different from that in finite size clusters. Several spectroscopic experiments[62,63] and ab initio calculations[64−70] have been performed to investigate the CTTS "precursor" states in clusters containing iodide and a small number of water molecules. Optimal geometries of iodide-water clusters correspond to a surface location of the ion and the water cluster possesses a relatively large dipole moment.[66,69] Consequently, the CTTS "precursor" has a character of a dipole bound state with a very diffuse wave function spreading outside the cluster. Another, energetically less favorable structure with iodine inside a water cluster (hexamer) has also been considered.[66,70] Again, in this case the electron promoted to the CTTS "precursor" state occupies space in the void, however, the corresponding wave function has a shape of a torus which is in a close contact with all the dangling water hydrogens. In any case, the CTTS "precursor" electrons in small water clusters are very fragile with a binding energy of less than 0.25 eV, compared to $\approx$ 1.5 eV binding in the extended liquid.[70] Clearly, most of the binding comes from the long-range polarization of a large number of water molecules by the (ground state) anion, an effect absent in small clusters.

B. Electron Photodetachment in Halide−water Clusters. For sufficiently short wavelengths, electrons can be directly photodetached from an aqueous halide anion using UV radiation. Provided the spectroscopic resolution is fine enough, information can be gained about the vibronic dynamics of the nascent neutral system directly after the electron photodetachment event. ZEKE spectroscopy is a technique which can provide 1 cm^{-1} resolution when applied to anionic clusters. So far, experiments have been performed for the smallest X^--H_2O (X = Cl, Br, and I) clusters.[75,109]

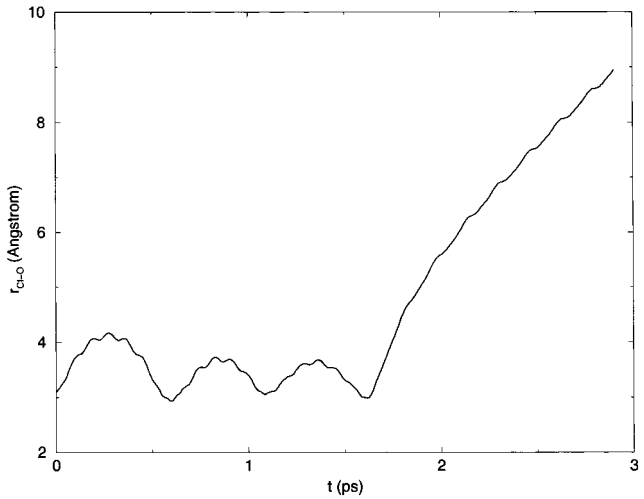

Figure 15. Time evolution of the Cl−O distance for a selected trajectory which corresponds to dissociation after three chlorine−water vibrations. The small undulations reflect the rapid internal rotation of the water molecule.

We have studied the ultrafast dynamics following photodetachment in Cl^--H_2O and Br^--H_2O clusters employing the method of Wigner trajectories.[77] In a one electron picture the photodetached electron leaves a p-hole in the halogen atom resulting in three quasi-degenerate potential energy surfaces (corresponding to the three possible orientations of the p-hole) split by the solvent and by the effect of spin−orbit coupling. We have constructed a diatomics-in-molecule fit to the ab initio (coupled cluster singles and doubles level) potential energy surfaces and have included spin−orbit interactions.[76,77] The early dynamics upon photodetachment is driven by the large difference between optimal cluster geometries for the anion and the neutral system. While the anion is strongly hydrogen bonded to one of the water hydrogens, the neutral halogen atom prefers a contact with the water oxygen, optimizing thus dispersion and polarization interactions.

Upon vertical photodetachment, the neutral halogen−water system is born in a repulsive region of the potential energy surface above the dissociation threshold. Two dynamical time scales can be distinguished: a fast one (≈70 fs), corresponding to an internal rotation of the water monomer, and a slow one (≈600 fs), which corresponds to an intermolecular halogen-water stretching vibration. Since a lot of the excess energy is initially deposited into water rotation, the cluster is unlikely to directly dissociate. Rather, several intermolecular vibrations with increasing amplitude are performed as the energy is transformed from rotations to vibrations, eventually leading to a delayed dissociation with a time constant of 5−10 ps. Figure 15 shows the time evolution of the Cl−O distance for one of the Wigner trajectories, illustrating the early dynamics of the nascent Cl^-H_2O cluster. We see that a typical pattern consists of several intermolecular vibrations followed eventually by cluster dissociation. Note that the small undulations on the curve correspond to fast internal rotations of the water molecule.

Most recently, we have similarly followed the early dynamics following electron photodetachment for a halide anion on clusters with 2−8 water molecules. In these larger clusters (possessing the heavier halide anion at the surface) several dissociation and fragmentation channels open and stabilization of a reduced size cluster by ejection of one or more water molecules is observed. Finally, to quantitatively model the ZEKE spectra the nuclear dynamics has to be described quantum mechanically. We are currently completing a 3D wave packet study of the dynamics following electron photodetachment in the $Cl^-−H_2O$ and $Br^-−H_2O$ clusters.

VII. Conclusions

The results reported in the present paper provide a unified picture of aqueous ionic solvation of simple salts at both cluster and bulk air/water interfaces. We have shown that polarizable ions such as the heavier halide anions have a propensity for the interface, with bromide and iodide exhibiting actually surfactant activity. This effect can be understood in terms of an additional stabilization that *polarizable ions* experience upon asymmetric solvation at the air/water interface. Traditional models of simple electrolytes fail to predict surface solvation because they neglect the effects of ion size and polarizability, and specific ion−water interactions.

The picture developed here follows from a combination of computational approaches, including high level ab initio quantum chemical calculations, and molecular dynamics simulations at finite temperature, based on both density functional and empirical polarizable potentials. The results obtained from these varying techniques were consistent in cases of overlap, i.e., for small water clusters containing a single salt or halide ion impurity. The cluster results presented here are in accord with numerous previous theoretical and direct experimental observations. The results for the bulk solution interfaces are supported indirectly by a number of experiments. However, direct experimental verification of the molecular details predicted by our calculations is highly desirable. In our study of anion adsorption in the series of sodium halide solutions,[83] we developed a detailed description of hydrogen bonding that could conceivably be tested by a surface sensitive vibrational spectroscopic measurement, such as vibrational sum frequency generation (VSFG).[110,111] Although the interpretation of these experiments in terms of molecular structure is not straightforward, it is possible to compute the spectra using MD simulation data,[112] and we imagine that a comparison of theoretical and experimental spectra could provide a definitive test of our predictions.

The presence of anions at aqueous interfaces is, among other things, relevant for the dynamics following photoexcitation of halide ions to charge-transfer-to-solvent states, and electron photodetachment. The results of this study also have direct implications for heterogeneous atmospheric chemistry. Reactions involving chloride anions at the surface of aqueous sea salt aerosols have been implicated in chlorine production in the marine boundary layer. The greater propensity of bromide versus chloride at the interface could explain the enhanced reactivity of bromide (despite its being present at much lower concentration in seawater) in the Arctic during polar sunrise.

Acknowledgment. We are grateful to our colleagues Barbara Finlayson-Pitts, John Hemminger, Benny Gerber, Steve Bradforth, and Martina Roeselova for stimulating discussions. Support from the Volkswagen Stiftung (Grant No. I/75908) and from the Czech Ministry of Education (Grant No. LN00A032) to P. J., and the National Science Foundation (Grant No. MCB-0078278) to D. J. T. is gratefully acknowledged.

References and Notes

(1) Adam, N. K. *The Physics and Chemistry of Surfaces*; Oxford University Press: London, 1941.

(2) Bikerman, J. J. *Surface Chemistry: Theory and Applications*; Academic Press: New York, 1958.

(3) Chattoraj, D. K.; Birdi, K. S. *Adsorption and the Gibbs Surface Excess*; Plenum: New York, 1984.

(4) Randles, J. E. B. *Phys. Chem. Liq.* **1977**, *7*, 107.
(5) Gibbs, J. W. *The Collected Works of J. W. Gibbs*; Longmans: Green, New York, 1931; Vol 1.
(6) Onsager, L.; Samaras, N. N. T. *J. Chem. Phys.* **1934**, *2*, 528.
(7) Benjamin, I. *J. Chem. Phys.* **1991**, *95*, 3698.
(8) Wilson, M. A.; Pohorille, A. *J. Chem. Phys.* **1991**, *95*, 6005.
(9) Xantheas, S. S. *J. Phys. Chem.* **1996**, *100*, 9703.
(10) Choi, J. H.; Kuwata, K. T.; Cao, Y. B.; Okumura, M. *J. Phys. Chem. A* **1998**, *102*, 503.
(11) Ayotte, P.; Weddle, G. H.; Kim, J.; Johnson, M. A. *J. Am. Chem. Soc.* **1998**, *120*, 12361.
(12) Ayotte, P.; Weddle, G. H.; Kim, J.; Johnson, M. A. *Chem. Phys.* **1998**, *239*, 485.
(13) Ayotte, P.; Bailey, C. G.; Weddle, G. H.; Johnson, M. A. *J. Phys. Chem. A* **1998**, *102*, 3067.
(14) Cabarcos, O. M.; Weinheimer, C. J.; Lisy, J. M.; Xantheas, S. S. *J. Chem. Phys.* **1999**, *110*, 5.
(15) Ayotte, P.; Weddle, G. H.; Johnson, M. A. *J. Chem. Phys.* **1999**, *110*, 7129.
(16) Ayotte, P.; Nielsen, S. B.; Weddle, G. H.; Johnson, M. A.; Xantheas, S. S. *J. Phys. Chem. A* **1999**, *103*, 10665.
(17) Dorsett, H. E.; Watts, R. O.; Xantheas, S. S. *J. Phys. Chem. A* **1999**, *103*, 3351.
(18) Wright, N. J.; Gerber, R. B. *J. Chem. Phys.* **2000**, *112*, 2598.
(19) Schenter, G. K.; Garrett, B. C.; Voth, G. A. *J. Chem. Phys.* **2000**, *113*, 5171.
(20) Perera, L.; Berkowitz, M. L. *J. Chem. Phys.* **1991**, *95*, 1954.
(21) Perera, L.; Berkowitz, M. L. *J. Chem. Phys.* **1992**, *96*, 8288.
(22) Perera, L.; Berkowitz, M. L. *J. Chem. Phys.* **1993**, *99*, 4222.
(23) Perera, L.; Berkowitz, M. L. *J. Chem. Phys.* **1993**, *100*, 3085.
(24) Sremaniak, L. S.; Perera, L.; Berkowitz, M. L. *Chem. Phys. Lett.* **1994**, *218*, 377.
(25) Yeh, I. C.; Perera, L.; Berkowitz, M. L. *Chem. Phys. Lett.* **1997**, *264*, 31.
(26) Dang, L. X.; Garrett, B. C. *J. Chem. Phys.* **1993**, *99*, 2972.
(27) Dang, L. X.; Smith, D. E. *J. Chem. Phys.* **1993**, *99*, 6950.
(28) Dang, L. X. *J. Chem. Phys.* **1999**, *110*, 1526.
(29) Stuart, S. J.; Berne, B. J. *J. Phys. Chem.* **1996**, *100*, 11934.
(30) Stuart, S. J.; Berne, B. J. *J. Phys. Chem. A* **1999**, *103*, 10300.
(31) Peslherbe, G. H.; Ladanyi, B. M.; Hynes, J. T. *Chem. Phys.* **2000**, *258*, 201.
(32) Markovich, G.; Giniger, R.; Levin, M.; Cheshnovsky, O. *J. Chem. Phys.* **1991**, *95*, 9416.
(33) Markovich, G.; Pollack, S.; Giniger, R.; Cheshnovsky, O. In *Reaction Dynamics in Clusters and Condensed Phases*; Jortner, J., Ed.; Kluwer: Amsterdam, 1994; p 13.
(34) Markovich, G.; Pollack, S.; Giniger, R.; Cheshnovsky, O. *J. Chem. Phys.* **1994**, *101*, 9344.
(35) Gora, R. W.; Roszak, S.; Leszczynski, J. *Chem. Phys. Lett.* **2000**, *325*, 7.
(36) Tobias, D. J.; Jungwirth, P.; Parrinello, M. *J. Chem. Phys.* **2001**, *114*, 7036.
(37) Jungwirth, P.; Tobias, D. J. *J. Phys. Chem. A*, **2002**, *106*, 379.
(38) Schlegel, H. B.; Millam, J. M.; Iyengar, S. S.; Voth, G. A.; Daniels, A. D.; Scuseria, G. E.; Frisch, M. J. *J. Chem. Phys.* **2001**, *114*, 9758.
(39) Iyengar, S. S.; Schlegel, H. B.; Millam, J. M.; Voth, G. A.; Scuseria, G. E.; Frisch, M. J. *J. Chem. Phys.* **2001**, *115*, 10291.
(40) Brdarski, S. Ph.D. Thesis, Lund University, Lund, 1999.
(41) Hu, J. H.; Shi, Q.; Davidovits, P.; Worsnop, D. R.; Zahniser, M. S.; Kolb, C. E. *J. Phys. Chem.* **1995**, *99*, 8768.
(42) Knipping, E. M.; Lakin, M. J.; Foster, K. L.; Jungwirth, P.; Tobias, D. J.; Gerber, R. B.; Dabdub, D.; Finlayson-Pitts, B. J. *Science* **2000**, *288* 301.
(43) Ghosal, S.; Shbeeb, A.; Hemminger, J. C. *Geophys. Res. Lett.* **2000**, *27*, 1879.
(44) Spicer, C. W.; Chapman, E. G.; Finlayson-Pitts, B. J.; Plastridge, R. A.; Hubbe, J. M.; Fast, J. D.; Berkowitz, C. M. *Nature* **1998**, *394*, 353.
(45) Oum, K. W.; Lakin, M. J.; DeHaan, D. O.; Brauers, T.; Finlayson-Pitts, B. J. *Science* **1998**, *279*, 74.
(46) Hirokawa, J.; Onaka, K.; Kajii, Y.; Akimoto, H. *Geophys. Res. Lett.* **1998**, *25*, 2449.
(47) Finlayson-Pitts, B. J.; Hemminger, J. C. *J. Phys. Chem. A* **2000**, *104*, 11463.
(48) von Glasow, R.; Sander, R. *Geophys. Res. Lett.* **2001**, *28*, 247.
(49) Andreae, M. O.; Crutzen, P. J. *Science* **1997**, *276*, 1052.
(50) Sander, R.; Rudich, Y.; von Glasow, R.; Crutzen, P. J. *Geophys. Res. Lett.* **1999**, *26*, 2857.
(51) Ravishankara, A. R. *Science* **1997**, *276*, 1058.
(52) Magi, L.; Schweitzer, F.; Pallares, C.; Cherif, S.; Mirabel, P.; George, C. *J. Phys. Chem. A* **1997**, *101*, 4943.
(53) Foster, K. L.; Plastridge, R. A.; Bottenheim, J. W.; Shepson, P. B.; Finlayson-Pitts, B. J.; Spicer, C. W. *Science* **2001**, *291*, 471.
(54) Oum, K. W.; Lakin, M. J.; Finlayson-Pitts, B. J. *Geophys. Res. Lett.* **1998**, *25*, 3923.
(55) Koop, T.; Kapilashrami, A.; Molina, L. T.; Molina, M. J. *J. Geophys. Res.* **2000**, *105*, 26393.
(56) Sander, R.; Crutzen, P. J. *J. Geophys. Res.* **1996**, *101*, 9121.
(57) Franck, J.; Schiebe, G. *Z. Phys. Chem.* **1928**, *139*, 22.
(58) Kloepfer, J. A.; Vilchitz, V. H.; Lenchenkov, V. A.; Bradforth, S. E. *Chem. Phys. Lett.* **1998**, *298*, 120.
(59) Kloepfer, J. A.; Vilchitz, V. H.; Lenchenkov, V. A.; Germaine, A. C.; Bradforth, S. E. *J. Chem. Phys.* **2000**, *113*, 6288.
(60) Vilchitz, V. H.; Kloepfer, J. A.; Germaine, A. C.; Lenchenkov, V. A.; Bradforth, S. E. *J. Phys. Chem. A* **2001**, *105*, 1711.
(61) Sheu, W.-S.; Rossky, P. J. *J. Phys. Chem.* **1996**, *100*, 1295.
(62) Serxner, D.; Dessent, C. E. H.; Johnson, M. A. *J. Chem. Phys.* **1996**, *105*, 7231.
(63) Lehr, L.; Zanni, M. T.; Frischkorn, C.; Weinkauf, R.; Neumark, D. M. *Science* **1999**, *284*, 635.
(64) Majumdar, D.; Kim, J.; Kim, K. S. *J. Chem. Phys.* **2000**, *112*, 101.
(65) Kim, J.; Lee, H. M.; Suh, S. B.; Majumdar, D.; Kim, K. S. *J. Chem. Phys.* **2000**, *113*, 5259.
(66) Chen, H.-Y.; Sheu, W.-S. *J. Am. Chem. Soc.* **2000**, *122*, 7534.
(67) Chen, H.-Y.; Sheu, W.-S. *Chem. Phys. Lett.* **2001**, *335*, 475.
(68) Waterland, M.; Myers-Kelley, A. *J. Phys. Chem. A* **2001**, *105*, 8385.
(69) Vila, F.; Jordan, K. D. *J. Phys. Chem. A* **2002**, *106*, 1391.
(70) Bradforth, S. E.; Jungwirth, P. *J. Phys. Chem. A* **2002**, *106*, 1286.
(71) Waller, I. M.; Kitsopoulos, T. N.; Neumark, D. M. *J. Phys. Chem.* **1990**, *94*, 2240.
(72) Gantefor, G.; Cox, D. M.; Kaldor, A. *J. Chem. Phys.* **1990**, *94*, 854.
(73) Muller-Detlefs, K.; Schlag, E. W. *Annu. Rev. Phys. Chem.* **1991**, *42*, 109.
(74) Drechsler, G.; Baessmannn, C.; Boesl, U.; Schlag, E. W. *J. Mol. Spectrosc.* **1995**, *348*, 337.
(75) Baessmannn, C.; Boesl, U.; Yang, D.; Drechsler, G.; Schlag, E. W. *Int. J. Mass Spectrosc. Ion Proc.* **1996**, *159*, 153.
(76) Roeselova, M.; Jacoby, G.; Kaldor, U.; Jungwirth, P. *Chem. Phys. Lett.* **1998**, *293*, 309.
(77) Roeselova, M.; Kaldor, U.; Jungwirth, P. *J. Phys. Chem. A* **2000**, *104*, 6523.
(78) Jungwirth, P. *J. Phys. Chem. A* **2000**, *104*, 145.
(79) Caldwell, J.; Dang, L. X.; Kollman, P. A. *J. Am. Chem. Soc.* **1990**, *112*, 9144.
(80) Markovich, G.; Perera, L.; Berkowitz, M. L.; Cheshnovsky, O. *J. Chem. Phys.* **1996**, *105*, 2675.
(81) Coker, H. *J. Phys. Chem.* **1976**, *80*, 2078.
(82) Pyper, N. C.; Pike, C. G.; Edwards, P. P. *Mol. Phys.* **1992**, *76*, 353.
(83) Jungwirth, P.; Tobias, D. J. *J. Phys. Chem. B* **2001**, *105*, 10468.
(84) Jungwirth, P.; Tobias, D. J. *J. Phys. Chem. B* **2000**, *104*, 7702.
(85) Essmann, U.; Perera, L.; Berkowitz, M. L.; Darden, T.; Pedersen, L. G. *J. Chem. Phys.* **1995**, *103*, 8577.
(86) Car, R,; Parrinello, M. *Phys. Rev. Lett.* **1985**, *55*, 2471.
(87) Kohn, W.; Sham, L. *Phys. Rev.* **1965**, *140*, 1133.
(88) Troullier, N.; Martins, J. *Phys. Rev. B* **1991**, *43*, 1993.
(89) Ramaniah, L. M.; Bernasconi, M.; Parrinello, M. *J. Chem. Phys.* **1998**, *109*, 6839.
(90) Ramaniah, L. M.; Bernasconi, M.; Parrinello, M. *J. Chem. Phys.* **1999**, *111*, 1587.
(91) Silvestrelli, P. L.; Parrinello, M. *J. Chem. Phys.* **1999**, *111*, 3572.
(92) Becke, A. D. *Phys. Rev. A* **1988**, *38*, 3098.
(93) Lee, C.; Yang, W.; Parr, R. C. *Phys. Rev. B* **1988**, *37*, 785.
(94) Silvestrelli, P. L.; Marzari, N.; Vanderbilt, D.; Parrinello, M. *Solid State Commun.* **1998**, *107*, 7.
(95) Berghold, G.; Mundy, C. J.; Romero, A. H.; Hutter, J.; Parrinello, M. *J. Chem. Phys.* **2000**, *61*, 10040.
(96) Gregoire, G.; Mons, M.; Dedonder-Lardeux, C.; Jouvet C. *Eur. Phys. J. D* **1998**, *1*, 5.
(97) Makov, G.; Nitzan, A. *J. Chem. Phys.* **1992**, *96*, 2965.
(98) Petersen, C. P.; Gordon, M. S. *J. Phys. Chem. A* **1999**, *103*, 4162.
(99) Bandyopadhyay, P.; Yoshikawa, A.; Gordon, M. S. In preparation.
(100) Lee, B.; Richards, F. M. *J. Mol. Biol.* **1971**, *55*, 379.
(101) Dang, L. X.; Chang, T. M. *J. Phys. Chem. A* **2002**, *106*, 235.
(102) Wingenter, O. W.; Blake, D. R.; Blake, N. J.; Sive, B. C.; Rowland, F. S. *J. Geophys. Res.* **1999**, *104*, 21819.
(103) Griffiths, F. B.; Bates, T. S.; Quinn, P. K.; Clementson, L. A.; Parslow, J. S. *J. Geophys. Res.* **1999**, *104*, 21649.
(104) Boudries, H.; Bottenheim, J. W. *Geophys. Res. Lett.* **2000**, *27*, 517.
(105) Ramacher, B.; Rudolph, J.; Koppmann, R. *J. Geophys. Res.* **1999**, *104*, 3633.
(106) Aryia, P. A.; Jobson, B. T.; Sander, R.; Niki, H.; Harris, G. W.; Hopper, J. F.; Anlauf, K. G. *J. Geophys. Res.* **1998**, *103*, 13.

(107) Watanabe, I.; Takahashi, N.; Tanida, H. *Chem. Phys. Lett.* **1998**, *287*, 714.
(108) Kohno, J.; Mafune, F.; Kondow, T. *J. Phys. Chem. A* **2001**, *105*, 5990.
(109) Boesl, U. Private communication.
(110) Schnitzer, C.; Baldelli, S.; Shultz, M. J. *J. Phys. Chem. B* **2000**, *104*, 585.
(111) Richmond, G. L. *Annu. Rev. Phys. Chem.* **2001**, *52*, 357.
(112) Morita, A.; Hynes, J. T. *Chem. Phys.* **2000**, *258*, 201.